Photocatalysis

DOI: 10.1002/ange.201407938

Sunlight-Driven Hydrogen Peroxide Production from Water and Molecular Oxygen by Metal-Free Photocatalysts**

Yasuhiro Shiraishi, Shunsuke Kanazawa, Yusuke Kofuji, Hirokatsu Sakamoto, Satoshi Ichikawa, Shunsuke Tanaka, and Takayuki Hirai*

Abstract: *Design of green, safe, and sustainable process for the synthesis of hydrogen peroxide (H_2O_2) is a very important subject. Early reported processes, however, require hydrogen (H_2) and palladium-based catalysts. Herein we propose a photocatalytic process for H_2O_2 synthesis driven by metal-free catalysts with earth-abundant water and molecular oxygen (O_2) as resources under sunlight irradiation ($\lambda > 400$ nm). We use graphitic carbon nitride (g-C_3N_4) containing electron-deficient aromatic diimide units as catalysts. Incorporating the diimide units positively shifts the valence-band potential of the catalysts, while maintaining sufficient conduction-band potential for O_2 reduction. Visible light irradiation of the catalysts in pure water with O_2 successfully produces H_2O_2 by oxidation of water by the photoformed valence-band holes and selective two-electron reduction of O_2 by the conduction band electrons.*

Hydrogen peroxide (H_2O_2) is a clean oxidant that emits only water as a byproduct and is widely used for pulp bleaching, disinfection, and organic synthesis.[1] H_2O_2 has also received much attention as an energy carrier for fuel cells, offering an alternative to H_2 because it is soluble in water and can be used in an one-compartment cell for electricity generation.[2] H_2O_2 is currently manufactured in industry by the anthraquinone method based on oxidation of anthrahydroquinone by O_2;[3] however, it requires a regeneration of anthrahydroquinone by hydrogenation of the formed anthraquinone with H_2 on palladium-based catalysts. Alternative to the high-energy-consuming two-step process, an one-step H_2O_2 synthesis with H_2 and O_2 has been studied extensively with Pd[4] or Au–Pd bimetallic catalysts.[5] This direct synthesis quantitatively produces H_2O_2, but requires extreme care because of the potentially explosive nature of H_2/O_2 mixed gases. A new method capable of producing H_2O_2 without H_2 is therefore desired.

Photocatalytic H_2O_2 production on semiconductor materials, such as titanium dioxide (TiO_2), has also been studied.[6] The reactions are usually carried out by UV irradiation ($\lambda <$ 400 nm) of an O_2-saturated water with TiO_2 in the presence of alcohols as the electron and proton donor. Photoexcitation of TiO_2 produces the electron (e^-) and positive hole (h^+) pairs. The h^+ oxidize alcohol and produce aldehyde and protons, while the e^- promote two-electron reduction of O_2 and produce H_2O_2 [Eq. (1) and (2)].

$$\text{R-CH}_2\text{OH} + 2\,h^+ \rightarrow \text{R-CHO} + 2\,H^+ \quad (1)$$

$$O_2 + 2\,H^+ + 2\,e^- \rightarrow H_2O_2 \quad (2)$$

These reactions proceed without H_2 at room temperature, therefore are a safe H_2O_2 synthesis. The selectivity for H_2O_2 formation is, however, very low (< 6 %). This is because one-electron reduction of O_2 occurs mainly and produces a superoxide ($^{\bullet}$OOH) radical [Eq. (3)],[7] thus suppressing two-electron reduction of O_2 [Eq. (2)].

$$O_2 + H^+ + e^- \rightarrow {}^{\bullet}\text{OOH} \quad (3)$$

Earlier, we found that graphitic carbon nitride (g-C_3N_4), a metal-free polymeric semiconductor with a graphitic stacking structure of melem sheets,[8] promotes selective two-electron reduction of O_2 and produces H_2O_2 with greater than 90 % selectivity under sunlight irradiation ($\lambda > 400$ nm).[9] The selective two-electron reduction of O_2 is due to the efficient formation of 1,4-endoperoxide species on the melem unit (Scheme 1). The photoformed e^- are localized at the C1 and N4 positions of melem (Scheme 1 a). The e^- reduces O_2 and creates a superoxo radical (Scheme 1 b). This is rapidly reduced by another e^- at the *para* position and produces 1,4-endoperoxide species (Scheme 1 c), which is readily transformed to H_2O_2. The rapid endoperoxide formation (Scheme 1 b→c) suppresses the $^{\bullet}$OOH radical formation [Scheme 1 b→d; Eq. (3)], thus promoting selective two-electron reduction of O_2 [Eq. (2)].

A green and sustainable process for photocatalytic H_2O_2 synthesis requires the use of earth-abundant water in place of alcohol. If this is achieved, oxidation of water by the photoformed h^+ produces O_2 and protons [Eq. (4)], while the e^- promote two-electron reduction of O_2 [Eq. (2)]. H_2O_2 can therefore be synthesized from water and O_2 under sunlight irradiation with 100 % atom efficiency [Eq. (5)].

$$2\,H_2O + 4\,h^+ \rightarrow O_2 + 4\,H^+ \quad (4)$$

[*] Dr. Y. Shiraishi, S. Kanazawa, Y. Kofuji, H. Sakamoto, Prof. T. Hirai
Research Center for Solar Energy Chemistry, and Division of Chemical Engineering, Graduate School of Engineering Science
Osaka University, Toyonaka 560-8531 (Japan)
E-mail: shiraish@cheng.es.osaka-u.ac.jp
Dr. S. Ichikawa
Institute for NanoScience Design
Osaka University (Japan)
Dr. S. Tanaka
Department of Chemical, Energy and Environmental Engineering
Kansai University (Japan)

[**] This work was supported by the Grant-in-Aid for Scientific Research (No. 26289296) from the Ministry of Education, Culture, Sports, Science and Technology (Japan) (MEXT).

Supporting information for this article is available on the WWW under http://dx.doi.org/10.1002/anie.201407938.

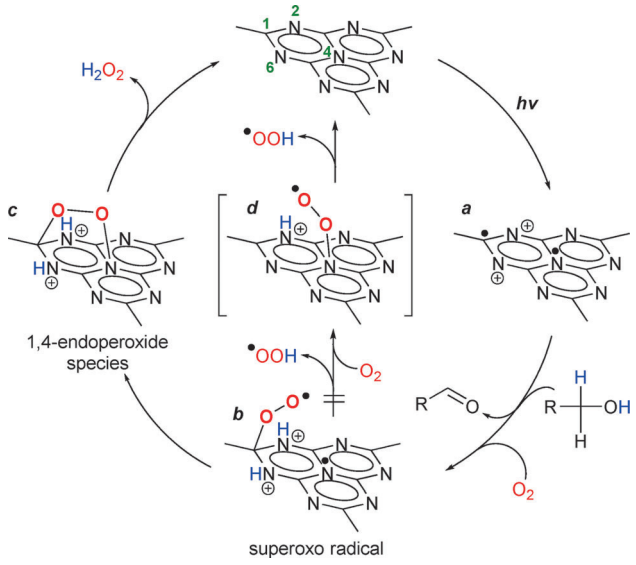

Scheme 1. Selective H_2O_2 production on g-C_3N_4 under visible light irradiation. For more details on (a)–(d) see text.

$$2\,H_2O + O_2 \rightarrow 2\,H_2O_2 \qquad (5)$$

The g-C_3N_4 catalyst is, however, unsuccessful for H_2O_2 production from water and O_2,[9] because the top of the valence band (VB) lies at approximately 1.4 V (versus the normal hydrogen electrode (NHE), pH 7),[10] which is insufficient for water oxidation (ca. 0.8 V)[11] because of the small thermodynamic driving force. Improving g-C_3N_4 to promote water oxidation while maintaining high selectivity for two-electron reduction of O_2 is necessary.

Herein we report that a simple modification of g-C_3N_4 facilitates H_2O_2 production from water and O_2. Aromatic diimides are an important class of n-type organic semiconductors for application to organic field-effect transistors (OFETs) owing to their high electron mobility and stability.[12] Incorporating the diimides into the semiconductors positively shifts the oxidation and reduction potentials due to their high electron affinity.[13] We incorporated pyromellitic diimide (PDI), a simple aromatic diimide, into the g-C_3N_4 network by a facile thermal condensation (Scheme 2). The obtained g-C_3N_4/PDI catalysts, when activated by visible light, successfully oxidize water owing to the positively shifted VB levels, while maintaining high selectivity for two-electron reduction of O_2. This thus facilitates H_2O_2 synthesis from water and O_2 under sunlight irradiation.

The g-C_3N_4/PDI_x catalysts containing different amounts of PDI units (x [mol %] = 33, 51, and 59) were prepared by calcinating a mixture of melem and pyromellitic dianhydride at 598 K (Scheme 2a), according to procedure for related materials.[14] As summarized in Table 1, the gray-brown powders of g-C_3N_4/PDI_x obtained have surface areas similar to g-C_3N_4 (5–8 $m^2 g^{-1}$). As shown in Figure S1 in the Support-

Table 1: Results for photocatalytic H_2O_2 production[a]

Entry	Catalyst	Surface area [$m^2 g^{-1}$][b]	H_2O_2 [μmol][c]
1	TiO_2[d]	57	< 0.2
2	Au/TiO_2[e]	-	< 0.2
3	F-TiO_2	-	< 0.2
4	g-C_3N_4	7.8	< 0.2
5	mpg-C_3N_4	190	< 0.2
6	g-C_3N_4/PDI_{33}	5.6	22.4
7	g-C_3N_4/PDI_{51}	7.1	50.6
	1st reuse[f]	-	50.2
	2nd reuse[f]	-	50.3
8	g-C_3N_4/PDI_{59}	6.7	39.4
9	*N,N'*-dipropylPDI[g]	-	< 0.2
10	g-C_3N_4 + *N,N'*-dipropylPDI[h]	-	< 0.2

[a] Reaction conditions: water (30 mL), catalyst (50 mg), O_2 (1 atm), $\lambda > 420$ nm (intensity at 420–500 nm: 26.9 $W m^{-2}$), time (48 h). [b] BET surface area. [c] Determined by redox titration with $KMnO_4$ (detection limit: 0.2 μmol). [d] JRC-TIO-4 TiO_2 supplied from the Catalyst Society of Japan (equivalent to Degussa P25; anatase/rutile = ca. 83/17). [e] The amount of Au loaded is 1 wt%, and the average diameter of Au particles is 3.4 ± 0.9 nm. [f] Catalyst was reused after simple washing with water followed by drying in vacuo. [g] 50 mg. [h] g-C_3N_4 (25 mg) and *N,N'*-dipropylPDI (25 mg).

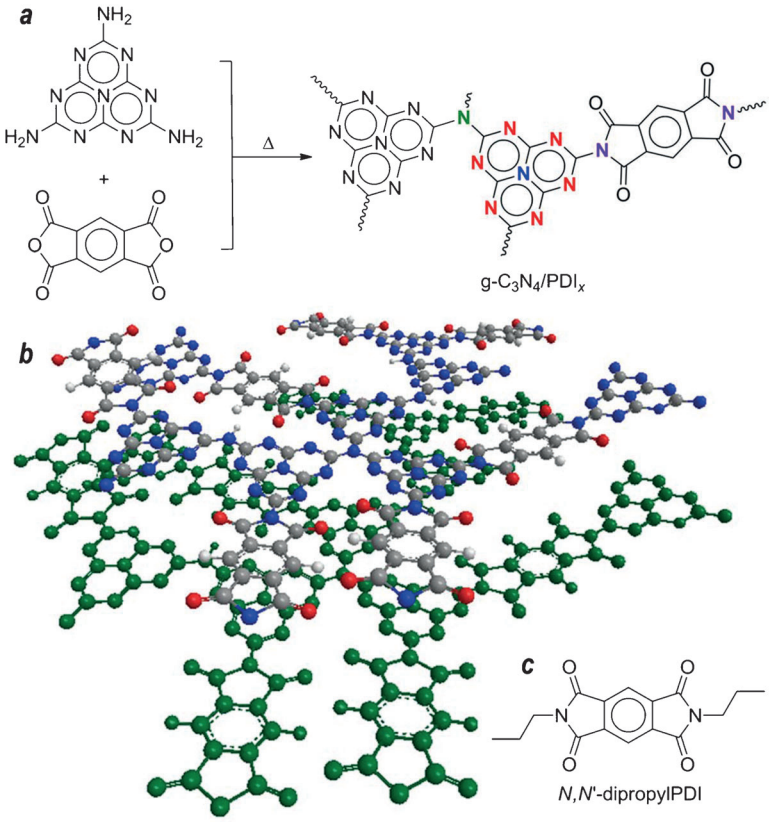

Scheme 2. a) Synthesis of g-C_3N_4/PDI_x, b) their proposed structure, and c) the structure of *N,N'*-dipropylPDI. C gray, H white, N blue, and O red spheres; the second layer is shown in green for clarity.

ing Information, transmission electron microscopy (TEM) images of the catalysts show sheet-like structures, as is the case for g-C_3N_4.[15] X-ray diffraction (XRD) of g-C_3N_4 (Figure S2) shows a peak at $2\theta = 27.4$ ($d = 0.325$ nm) assigned to (002) packing of the melem sheets.[16] Increasing the amounts of PDI units decreases its intensity, along with a formation of new two peaks at $2\theta = 19.0$ ($d = 0.467$ nm) and 29.6 ($d = 0.302$ nm). These are assigned to π,π-stacking of PDI units[17] and donor–acceptor interaction between melem and PDI units,[18] respectively. These data suggest that, as shown in Scheme 2b, the PDI units are randomly incorporated within the melem sheet and the sheets are layered multiply. As shown in Figure S3, X-ray photoelectron spectroscopy (XPS) of g-C_3N_4 (N1s level) shows three peaks assigned to sp^2-hybridized N atoms of melem at 398.5 eV (red, Scheme 2a), trigonal N atoms of the melem center at 399.4 eV (blue, Scheme 2a), and terminal amine N atoms at 401.0 eV (green, Scheme 2a), respectively.[19] Incorporating PDI units creates a new peak at 400.1 eV, assigned to imide N atoms of the PDI units (purple, Scheme 2).[20] Integrating these signals therefore allows rough determination of the mole fraction of PDI units (x) within g-C_3N_4/PDI_x.

Diffuse-reflectance UV/Vis spectra of g-C_3N_4/PDI_x (Figure S4) show absorption in the visible region, as is the case for g-C_3N_4; their band-gap energies are 2.4–2.8 eV. Electrochemical Mott–Schottky plots of g-C_3N_4/PDI_x (Figure S5) show typical n-type character. The obtained flat band potentials and band-gap energies provide the band structures of g-C_3N_4/PDI_x (Figure 1). Both conduction band (CB) and VB levels

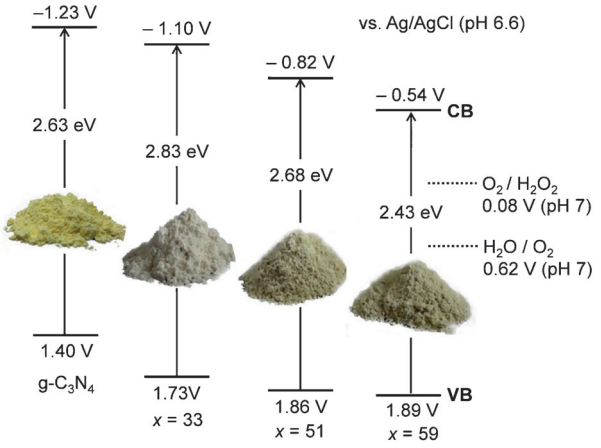

Figure 1. Electronic band structures of g-C_3N_4 and g-C_3N_4/PDI_x. Photographs show the corresponding powders of the samples.

become more positive by the incorporation of PDI units owing to their high electron affinity,[13] with the CB levels still more negative than the reduction potential of O_2 (0.08 V).[11] These data suggest that g-C_3N_4/PDI_x may possess enhanced capability for water oxidation with sufficient potentials for O_2 reduction.

Photocatalytic reactions were performed by photoirradiation of pure water (30 mL) containing respective catalysts (50 mg) by a Xe lamp ($\lambda > 420$ nm) with magnetic stirring under O_2 atmosphere (1 atm) at 298 K. Table 1 summarizes the results obtained by 48 h reaction. Bare TiO_2 (entry 1) scarcely produces H_2O_2 (less than detection limit, 0.2 μmol). TiO_2 loaded with Au[6f] or modified with fluoride,[6d] which have been proposed for H_2O_2 production, are inactive (entries 2 and 3). g-C_3N_4 (entry 4) does not produce H_2O_2. Mesoporous g-C_3N_4 (mpg-C_3N_4) with a large surface area (190 $m^2 g^{-1}$) prepared by a silica-templated polymerization[21] is also inactive (entry 5). In contrast, g-C_3N_4/PDI_x produce very large amounts of H_2O_2 (entries 6–8); the amount of H_2O_2 formed on g-C_3N_4/PDI_{51} (50.6 μmol) is more than 250-fold of that obtained with g-C_3N_4 (< 0.2 μmol). As shown by entries 9 and 10, *N*,*N*′-dipropylPDI (Scheme 2c), a reference compound for PDI, and a mixture of g-C_3N_4 and *N*,*N*′-dipropylPDI scarcely produces H_2O_2. These data suggest that incorporating PDI units within the g-C_3N_4 network facilitates H_2O_2 production from water and O_2.

Table S1 shows the results of photoreaction on g-C_3N_4/PDI_x with 2-PrOH as a sacrificial electron donor. The selectivity for the amount of H_2O_2 formed relative to the amounts of photooxidation products (acetone and CO_2) is about 90%, which is similar to that obtained with g-C_3N_4. This suggests that g-C_3N_4/PDI_x selectively promote two-electron reduction of O_2 as does g-C_3N_4.[9] Figure S6 shows the change in the amounts of H_2O_2 formed during reaction in a water/O_2 system with g-C_3N_4/PDI_x. The rate of H_2O_2 evolution is almost constant even after prolonged irradiation, indicating that the catalysts produce H_2O_2 without loss of activity. The g-C_3N_4/PDI_{51} catalyst, when reused for further reaction (entry 7, Table 1), shows almost the same activity as the fresh sample. In addition, the recovered catalyst shows similar X-ray diffraction (XRD) pattern to that of the fresh one (Figure S2). These data suggest that the catalyst is stable and reusable for further reaction.

Figure S7 shows the action spectrum[22] for H_2O_2 formation on g-C_3N_4/PDI_{51}. The apparent quantum yields (Φ_{AQY}) agree with the absorption spectrum of the catalyst, indicating that its band-gap excitation promotes water oxidation and O_2 reduction. Note that Φ_{AQY} at 420 nm is 2.6%, which is similar to that for overall water splitting on a highly active solid-solution catalyst (ca. 2.5% at 420 nm).[23] Ab initio calculations based on the density functional theory (DFT) were performed within the Gaussian 03 program to clarify the effect of PDI unit on the electronic structure of g-C_3N_4 with simple melem and melem-PDI models (Figure 2). Their main electronic transitions ($S_0 \rightarrow S_1$) are HOMO→LUMO and HOMO→LUMO + 2, respectively. Incorporating PDI units decreases both S_0 and S_1 levels; this agrees with the observed VB and CB levels (Figure 1). The electrons on both HOMO and LUMO + 2 of the melem-PDI model are located mainly at the melem unit with partial distribution to the PDI units. This is reflected by the high electron affinity of PDI unit.[13] The electrons on HOMO are located at the N2 and N6 positions of the melem unit, and those on LUMO + 2 are at the C1 and N4 units. These data suggest that these respective atoms on the melem units behave as the oxidation (N2 and N6) and reduction (C1 and N4) sites, as is the case for g-C_3N_4[9] (Scheme 1).

The mechanism for H_2O_2 formation on the photoexcited g-C_3N_4/PDI can be explained as Scheme 3.[24] Photoexcitation

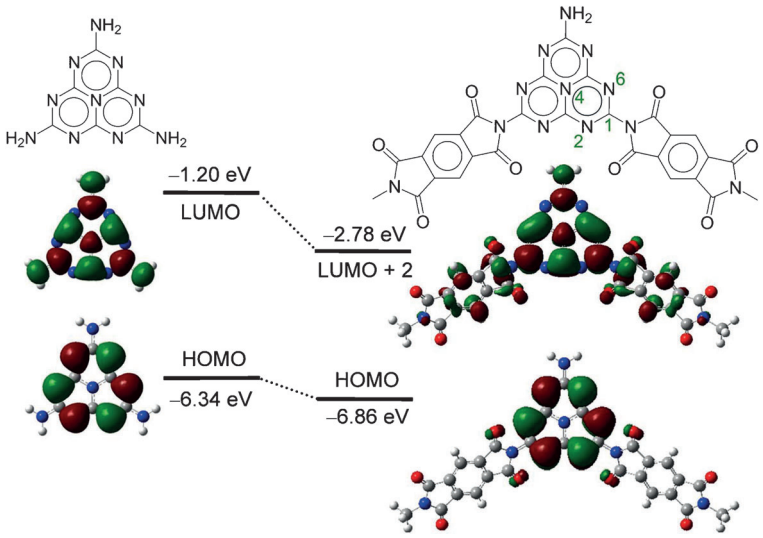

Figure 2. Energy diagrams and interfacial plots of main orbitals for melem (left) and melem-PDI (right) models calculated at the DFT level (B3LYP/6-31g(d)).

by two photons creates two sets of e^-/h^+ pairs (Scheme 3a). The formed e^- are localized at the C1 and N4 positions of the melem unit, whereas h^+ are at the N2 and N6 positions. The h^+ oxidizes water (Scheme 3b), and the e^- on either C1 or N4 position reduces O_2, producing a superoxo radical (Scheme 3c). This radial is rapidly reduced by the e^- at the *para* position, producing 1,4-endoperoxide species (Scheme 3d). Protonation of the species produces H_2O_2.

The 1,4-endoperoxide formation on g-C_3N_4/PDI (Scheme 3d) is confirmed by Raman spectroscopy. As shown in Figure 3A, fresh g-C_3N_4/PDI_{51} exhibits four bands at 645, 709, 753, and 982 cm^{-1}. The 645 cm^{-1} band is assigned to in-plane bending mode of imide moiety.[25] Both the 709 and 982 cm^{-1} bands are assigned to breathing mode of melem, and the 753 cm^{-1} band is assigned to out-of-plane bending mode of melem.[26] Figure 3a shows the Raman shift of the melem-PDI model obtained by DFT calculation. The four bands obtained (619, 665, 766, and 1004 cm^{-1}) are similar to the observed ones (Figure 3A), indicating that the calculation precisely represents the electronic structure of g-C_3N_4/PDI. Figure 3B shows the Raman spectrum of g-C_3N_4/PDI_{51} recovered after photoreaction in a 2-PrOH/O_2 system. A new broad band appears at 892 cm^{-1}. Figure 3b depicts the calculated Raman shift of 1,4-endoperoxide species adsorbed on the melem-PDI system. The three bands obtained (837, 890, and 906 cm^{-1}) are assigned to the C1–O symmetric, O–O stretching, and C1–O asymmetric vibrations of the endoperoxide species, respectively. They agree reasonably with the observed broad band at 892 cm^{-1} (Figure 3B). Figure 3C shows the Raman spectrum of g-C_3N_4 recovered after photoreaction. A similar band appears at 891 cm^{-1}, assigned to the 1,4-endoperoxide species. These data indicate that two-electron reduction of O_2 is indeed promoted on the g-C_3N_4/PDI surface (Scheme 3).

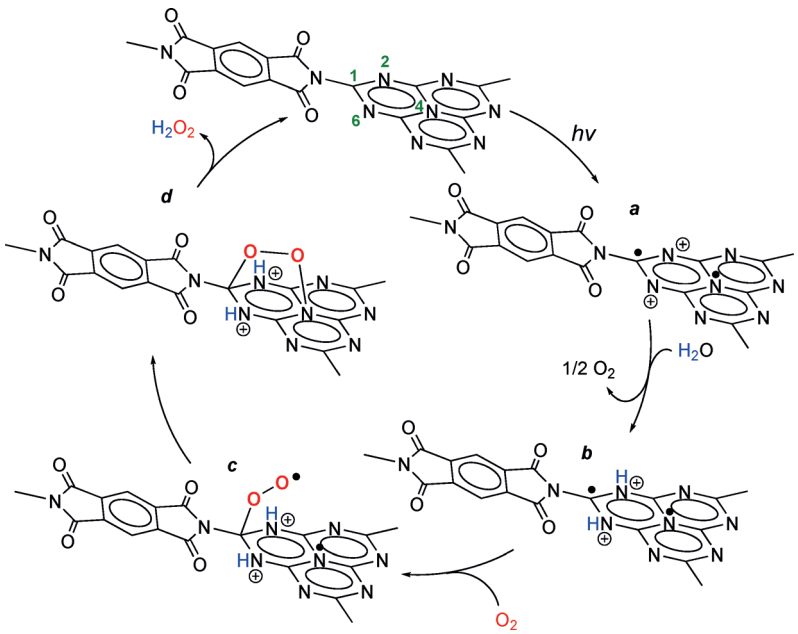

Scheme 3. Proposed mechanism for H_2O_2 formation on the photoactivated g-C_3N_4/PDI from water and O_2.[24] For more details on (a)–(d) see text.

The activity of H_2O_2 formation increases with the incorporation of PDI units (Table 1). The reaction consists of water oxidation and O_2 reduction. To clarify the activity of these half reactions, water oxidation with $AgNO_3$ as an electron acceptor and O_2 reduction with 2-PrOH as an electron donor were carried out. As shown in Figure S8 and S9, the activity of both reactions increases with the amount of PDI units. The rate of water oxidation with $AgNO_3$ on g-C_3N_4/PDI_{51} is 0.8 μmol h^{-1}. This is much smaller than that of O_2 reduction with 2-PrOH (42 μmol h^{-1}) but similar to that of H_2O_2 formation in a water/O_2 system (1.1 μmol h^{-1}, Figure S6). This result suggests that water oxidation is the rate-determining step for H_2O_2 formation. The positive shift of the VB level by incorporating PDI units (Figure 1) therefore facilitates water oxidation and promotes H_2O_2 formation.

Of the catalysts, g-C_3N_4/PDI_{51} shows the highest activity (Table 1). The catalyst containing a larger amount of PDI units (g-C_3N_4/PDI_{59}) shows decreased activity despite its more positive VB level. The half reactions show similar tendency of the activity (Figure S8 and S9). As shown in Figure 1, incorporating PDI units also positively shifts the CB level. One of the possible reasons for the low activity is therefore the insufficient reduction capability. In addition, as shown in Scheme 3, the melem unit acts as the active sites for both water oxidation and O_2 reduction. Incorporating larger amounts of PDI units decreases the number of melem units exposed on the catalyst. This may be another possible reason for the low activity. The g-C_3N_4/

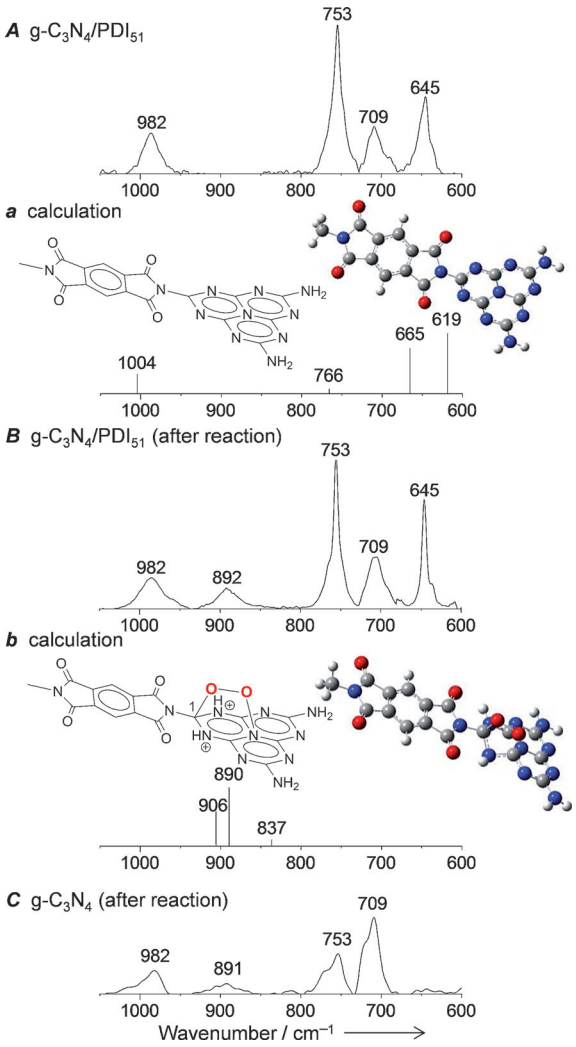

Figure 3. Raman spectra for A) fresh g-C_3N_4/PDI_{51}, and B) g-C_3N_4/PDI_{51} recovered after photoreaction, and C) g-C_3N_4 recovered after photoreaction (12 h) in a 2-PrOH solution with O_2. Calculated shift for a) the melem-PDI model and b) the model with 1,4-endoperoxide species (B3LYP/6-31g(d)).

PDI_{51} catalyst has appropriate VB and CB levels and relatively large number of active sites (melem units), thus facilitating efficient H_2O_2 production.

Efficient H_2O_2 formation on g-C_3N_4/PDI requires visible light irradiation ($\lambda > 400$ nm); UV irradiation decreases the efficiency. Photoreaction with a solar simulator as a light source confirms this. As shown in Figure 4a, spectral irradiance of the simulator (Figure 4a, orange) ranges from UV to visible region and is similar to that of sunlight (Figure 4a, green). Figure 4b shows the time-dependent change in H_2O_2 evolution with g-C_3N_4/PDI_{51} in a water/O_2 system under irradiation by a solar simulator. Irradiation of entire wavelength light (Figure 4b, orange) successfully produces H_2O_2 at the early stage, but the formation rate decreases with time. This is due to the decomposition of the formed H_2O_2 by absorbing UV light ($\lambda < 400$ nm).[9,27,28] In contrast, irradiation of $\lambda > 420$ nm light using a glass filter (Figure 4b, blue) produces H_2O_2 without a decrease in the formation rate.

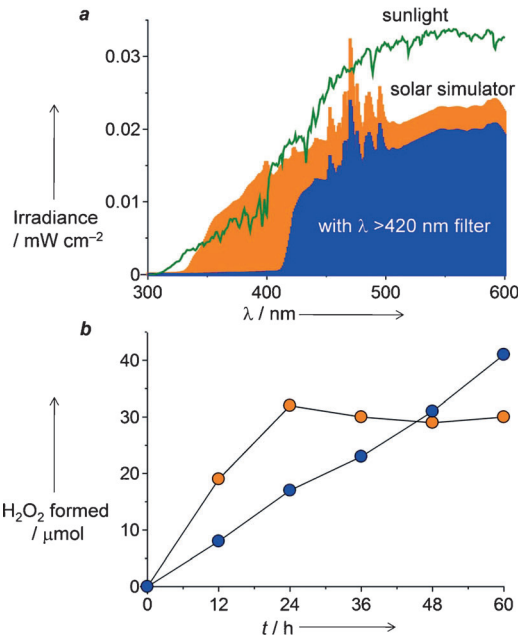

Figure 4. a) Spectral irradiance for sunlight (green, Nov 23, 2013 at 8:00–17:00, north latitude 34.7°, east longitude 135.5°; light intensity at 300–500 nm, 2.8 mW cm^{-2}) and solar simulator (orange) without and (blue) with $\lambda > 420$ nm filter (light intensity at 300–500 nm and 420–500 nm are 2.9 and 1.3 mW cm^{-2}, respectively). b) Time-dependent change in H_2O_2 evolution during photoreaction with g-C_3N_4/PDI_{51} in a water/O_2 system under irradiation by solar simulator (orange) without and (blue) with $\lambda > 420$ nm filter.

These data suggest that g-C_3N_4/PDI is successfully activated by visible region light within sunlight and promotes efficient H_2O_2 production.

In summary, we found that sunlight activation of g-C_3N_4/PDI produces H_2O_2 from water and O_2. This promotes water oxidation and two-electron reduction of O_2, facilitating efficient production of H_2O_2. At present, the catalytic activity is insufficient; the amount of H_2O_2 formed by 48 h reaction is approximately 30 μmol (1 mM). Activity improvement is necessary for practical application. Nevertheless, the present photoprocess has significant advantages: 1) metal-free catalyst, 2) cost-free light (sunlight), 3) earth-abundant resources (water and O_2), and 4) mild reaction conditions (atmospheric pressure and ambient temperature). The basic concept presented herein based on the band engineering of g-C_3N_4 with aromatic diimide may contribute to the design of safe, green, and sustainable H_2O_2 synthesis by sunlight.

Received: August 4, 2014
Published online: October 7, 2014

Keywords: graphitic carbon nitride · hydrogen peroxide · oxygen · photocatalysis · water

[1] J. M. Campos-Martin, G. Blanco-Brieva, J. L. G. Fierro, *Angew. Chem. Int. Ed.* **2006**, *45*, 6962–6984; *Angew. Chem.* **2006**, *118*, 7116–7139.
[2] A. E. Sanli, A. Aytac, *Int. J. Hydrogen Energy* **2011**, *36*, 869–875.

[3] F. Sandelin, P. Oinas, T. Salmi, J. Paloniemi, H. Haario, *Ind. Eng. Chem. Res.* **2006**, *45*, 986 – 992.
[4] a) D. Gudarzi, W. Ratchananusorn, I. Turunen, T. Salmi, M. Heinonen, *Top. Catal.* **2013**, *56*, 527 – 539; b) S. Melada, R. Rioda, F. Menegazzo, F. Pinna, G. Strukul, *J. Catal.* **2006**, *239*, 422 – 430.
[5] a) J. K. Edwards, B. E. Solsona, P. Landon, A. F. Carley, A. Herzing, C. J. Kiely, G. J. Hutchings, *J. Catal.* **2005**, *236*, 69 – 79; b) J. C. Pritchard, Q. He, E. N. Ntainjua, M. Piccinini, J. K. Edwards, A. A. Herzing, A. F. Carley, J. A. Moulijn, C. J. Kiely, G. J. Hutchings, *Green Chem.* **2010**, *12*, 915 – 921.
[6] a) C. Kormann, D. W. Bahnemann, M. R. Hoffmann, *Environ. Sci. Technol.* **1988**, *22*, 798 – 806; b) R. Cai, Y. Kubota, A. Fujishima, *J. Catal.* **2003**, *219*, 214 – 218; c) H. Goto, Y. Hanada, T. Ohno, M. Matsumura, *J. Catal.* **2004**, *225*, 223 – 229; d) V. Maurino, C. Minero, G. Mariella, E. Pelizzetti, *Chem. Commun.* **2005**, 2627 – 2629; e) T. Hirakawa, Y. Nosaka, *J. Phys. Chem. C* **2008**, *112*, 15818 – 15823; f) M. Teranishi, S. Naya, H. Tada, *J. Am. Chem. Soc.* **2010**, *132*, 7850 – 7851; g) D. Tsukamoto, A. Shiro, Y. Shiraishi, Y. Sugano, S. Ichikawa, S. Tanaka, T. Hirai, *ACS Catal.* **2012**, *2*, 599 – 603.
[7] Y. Shiraishi, S. Kanazawa, D. Tsukamoto, A. Shiro, Y. Sugano, T. Hirai, *ACS Catal.* **2013**, *3*, 2222 – 2227.
[8] a) X. Wang, K. Maeda, A. Thomas, K. Takanabe, G. Xin, J. M. Carlsson, K. Domen, M. Antonietti, *Nat. Mater.* **2009**, *8*, 76 – 80; b) A. Thomas, A. Fischer, F. Goettmann, M. Antonietti, J. O. Müller, R. Schlögl, J. M. Carlsson, *J. Mater. Chem.* **2008**, *18*, 4893 – 4908.
[9] Y. Shiraishi, S. Kanazawa, Y. Sugano, D. Tsukamoto, H. Sakamoto, S. Ichikawa, T. Hirai, *ACS Catal.* **2014**, *4*, 774 – 780.
[10] Y. Cui, Z. Ding, P. Liu, M. Antonietti, X. Fu, X. Wang, *Phys. Chem. Chem. Phys.* **2012**, *14*, 1455 – 1462.
[11] a) J. Chen, P. Wagner, L. Tong, G. G. Wallace, D. L. Officer, G. F. Sweigers, *Angew. Chem. Int. Ed.* **2012**, *51*, 1907 – 1910; *Angew. Chem.* **2012**, *124*, 1943 – 1946; b) W. H. Koppenol, *J. Am. Chem. Soc.* **2007**, *129*, 9686 – 9690.
[12] a) Q. Zheng, J. Huang, A. Sarjeant, H. E. Katz, *J. Am. Chem. Soc.* **2008**, *130*, 14410 – 14411; b) Z. Wang, C. Kim, A. Facchetti, T. J. Marks, *J. Am. Chem. Soc.* **2007**, *129*, 13362 – 13363; c) T. J. Dingemans, S. J. Picken, N. S. Murthy, P. Mark, T. L. St Clair, E. T. Samulski, *Chem. Mater.* **2004**, *16*, 966 – 974.
[13] a) C. Hu, Q. Zhang, *Polym. Bull.* **2012**, *69*, 63 – 69; b) K. Bijak, M. G. Zajac, H. Janeczek, M. Wiacek, E. S. Balcerzak, *Synth. Met.* **2013**, *175*, 146 – 154; c) S. Chu, Y. Wang, Y. Guo, J. Feng, C. Wang, W. Luo, X. Fan, Z. Zou, *ACS Catal.* **2013**, *3*, 912 – 919.
[14] a) F. Xiao, K. Wang, M. Zhan, *Appl. Surf. Sci.* **2010**, *256*, 7384 – 7388; b) S. R. Puniredd, M. P. Srinivasan, *Langmuir* **2005**, *21*, 7812 – 7822.
[15] H. Xu, J. Yan, Y. Xu, Y. Song, H. Li, J. Xia, C. Huang, H. Wan, *Appl. Catal. B* **2013**, *129*, 182 – 193.
[16] H. Ji, F. Chang, X. Hu, W. Qin, J. Shen, *Chem. Eng. J.* **2013**, *218*, 183 – 190.
[17] Q. Bao, B. M. Goh, B. Yan, T. Yu, Z. Shen, K. P. Loh, *Adv. Mater.* **2010**, *22*, 3661 – 3666.
[18] L. Xue, Y. Wang, Y. Chen, X. Li, *J. Colloid Interface Sci.* **2010**, *350*, 523 – 529.
[19] H. Dai, X. Gao, E. Liu, Y. Yang, W. Hou, L. Kang, J. Fan, X. Hu, *Diamond Relat. Mater.* **2013**, *38*, 109 – 117.
[20] Z. Qin, J. Zhang, H. Zhou, Y. Song, T. He, *Nucl. Instrum. Methods Phys. Res. Sect. B* **2000**, *170*, 406 – 412.
[21] X. Wang, K. Maeda, X. Chen, K. Takanabe, K. Domen, Y. Hou, X. Fu, M. Antonietti, *J. Am. Chem. Soc.* **2009**, *131*, 1680 – 1681.
[22] Y. Sugano, Y. Shiraishi, D. Tsukamoto, S. Ichikawa, S. Tanaka, T. Hirai, *Angew. Chem. Int. Ed.* **2013**, *52*, 5295 – 5299; *Angew. Chem.* **2013**, *125*, 5403 – 5407.
[23] K. Maeda, K. Teramura, D. Lu, T. Takata, N. Saito, Y. Inoue, K. Domen, *Nature* **2006**, *440*, 295.
[24] A two-electron process involving simultaneous formation of two e^-/h^+ pairs and their consumption is tentatively proposed in Scheme 3, although water oxidation is a four-electron process and occurs in a stepwise manner. This is because, at the present stage, the position of another two e^-/h^+ pairs on the melem unit and the mechanism for O_2 formation are unclear.
[25] W. H. Tsai, F. J. Boerio, K. M. Jackson, *Langmuir* **1992**, *8*, 1443 – 1450.
[26] a) P. V. Zinin, L. C. Ming, S. K. Sharma, V. N. Khabashesku, X. Liu, S. Hong, S. Endo, T. Acosta, *Chem. Phys. Lett.* **2009**, *472*, 69 – 73; b) D. Papadimitriou, G. Roupakas, C. A. Dimitriadis, S. Logothetidis, *J. Appl. Phys.* **2002**, *92*, 870 – 875.
[27] S. Goldstein, D. Aschengrau, Y. Diamant, J. Rabani, *Environ. Sci. Technol.* **2007**, *41*, 7486 – 7490.
[28] This is confirmed by photoirradiation of a water (30 mL) with H_2O_2 (100 μmol) under Ar. The rate of H_2O_2 decomposition under >300 nm irradiation is 4.5 $\mu mol\,h^{-1}$, which is similar to that obtained with 50 mg g-C_3N_4/PDI_{51} (4.8 $\mu mol\,h^{-1}$). In contrast, the decomposition rates under >420 nm irradiation without and with catalyst are 0.5 and 0.7 $\mu mol\,h^{-1}$, respectively. These data indicate that photocatalytic decomposition of H_2O_2 scarcely occurs and direct decomposition by absorbing UV light is the crucial factor for H_2O_2 decomposition.

